A Theoretical Study of Unimolecular Reactions of Dimethyl Persulfoxide

Michael L. McKee

Contribution from the Department of Chemistry, Auburn University, Auburn, Alabama 36849

Received August 27, 1997. Revised Manuscript Received March 5, 1998

Abstract: Unimolecular reactions on the $(CH_3)_2SOO$ potential energy surface have been calculated in an attempt to rationalize the reaction of singlet oxygen with dimethyl sulfide. Geometries were optimized with B3LYP/6-31+G(d) except for $(CH_3)_2SOO$ which is not correctly described at that level of theory. Single-point calculations were made with a computational scheme similar to G2(MP2,SVP). A second intermediate, $CH_3S(CH_2)OOH$, formed by intramolecular hydrogen abstraction ($\Delta H_a = 4.8$ kcal/mol), is found to play a pivotal role in the concerted reaction pathway. From this intermediate, dimethyl sulfone can be formed in two steps. First, a hydroxyl group migrates to the sulfur ($\Delta H_a = 8.3$ kcal/mol) followed by intramolecular hydrogen migration to the methylene group ($\Delta H_a = 14.4$ kcal/mol). Alternatively, the $CH_3S(CH_2)(O)OH$ intermediate can be protonated by trace water and deprotonated to form dimethyl sulfone, which can explain the H/D exchange process observed experimentally. A sulfurane, formed by the addition of water to $(CH_3)_2SOO$, is calculated to be bound by 13.5 kcal/mol.

Introduction

The first step in the oxidation of sulfides by singlet dioxygen is the formation of a zwitterionic persulfoxide known as the primary intermediate (PI).[1−7] In the mechanism proposed by Foote and co-workers (Scheme 1),[1−3,8] the PI can react directly with sulfoxides to produce sulfones or can undergo a transformation to a secondary intermediate (SI) which can be trapped with sulfides to form sulfoxides (but not sulfones). Since the SI oxidizes sulfides electrophilically, it is possible that the SI is thiadioxirane.[9,10] While the sulfones produced in Scheme 1 are formed in a bimolecular step, $^{16}O_2/^{18}O_2$ labeling studies indicate that sulfones can also be produced by unimolecular rearrangement.[4,5,11,12]

Sulfides bearing an active α-CH bond (such as dibenzylsulfide) are known to undergo C−S cleavage to form an aldehyde plus sulfenic acid (Scheme 2) as well as the usual sulfoxide and sulfone products.[4,5,13] Although not isolated, possible intermediates in the formation of the aldehyde would be *S*-hydroperoxysulfonium ylides (**A**) and α-hydroperoxysulfide (**B**).[12,14] The reaction of dibenzyl sulfide with TAD (1,2,4-triazoline-3,5-dione), rather than singlet oxygen (Scheme 2), yields a product analogous to α-hydroperoxysulfide (**B′**).[15] This fact supports the postulated intermediate **B** in the reaction of dibenzyl sulfide with singlet oxygen.

Sulfur−carbon cleavage products are also observed in the photooxidation of the five-membered-ring sulfide, but not of the cyclic six- or seven-membered-ring sulfides or the acyclic dialkyl sulfides.[4] It was pointed out that the α-protons are more acidic in the five-membered rings, which might favor the formation of the *S*-hydroperoxysulfonium ylide intermediate (**A**, Scheme 2).

Scheme 1

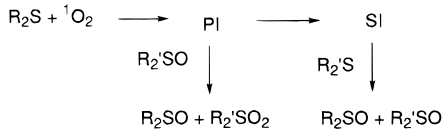

Scheme 2

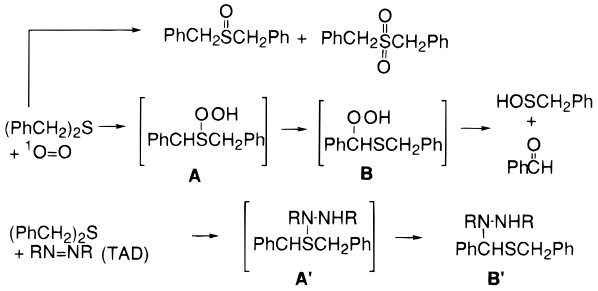

(1) Foote, C. S.; Peters, J. W. *J. Am. Chem. Soc.* **1971**, *93*, 3795.
(2) (a) Gu, C.-L.; Foote, C. S. *J. Am. Chem. Soc.* **1982**, *104*, 6060. (b) Liang, J.-J.; Gu, C.-L.; Kacher, M. L.; Foote, C. S. *J. Am. Chem. Soc.* **1983**, *105*, 4717.
(3) (a) Jensen, F. In *Advances in Oxygenated Processes*; Baumstark, A. L., Ed.; JAI Press: Greenwich, CT, 1995; Vol. IV, pp 1−49. (b) Jensen, F.; Greer, A.; Clennan, E. L. *J. Am. Chem. Soc.* In press.
(4) Clennan, E. L. In *Advances in Oxygenated Processes*; Baumstark, A. L., Ed.; JAI Press: Greenwich, CT, 1995; Vol IV, pp 49−80.
(5) Ando, W.; Takata, T. In *Singlet O_2: Reactions Modes and Products*; Frimer, A. A., Ed.; CRC Press: Boca Raton, 1985; Vol 3, Part 2.
(6) Akasaka, T.; Yabe, A.; Ando, W. *J. Am. Chem. Soc.* **1987**, *109*, 8085.
(7) Clennan, E. L.; Oolman, K. A.; Yang, K.; Wang, D.-X. *J. Org. Chem.* **1991**, *56*, 4286.
(8) Jensen, F.; Foote, C. S. *J. Am. Chem. Soc.* **1988**, *110*, 2368.
(9) Watanabe, Y.; Kuriki, N.; Ishiguro, K.; Sawaki, Y. *J. Am. Chem. Soc.* **1991**, *113*, 2677.
(10) Greer, A.; Jensen, F.; Clennan, E. L. *J. Org. Chem.* **1996**, *61*, 4107.
(11) Clennan, E. L.; Zhang, H. *J. Org. Chem.* **1994**, *59*, 7952.
(12) Ishiguro, K.; Hayashi, M.; Sawaki, Y. *J. Am. Chem. Soc.* **1996**, *118*, 7265.
(13) Akasaka, T.; Sakurai, A.; Ando, W. *J. Am. Chem. Soc.* **1991**, *113*, 2696.
(14) Greer, A.; Chen, M.-F.; Jensen, F.; Clennan, E. L. *J. Am. Chem. Soc.* **1997**, *119*, 4380.
(15) Ando, W.; Ito, K.; Takata, T. *Tetrahedron Lett.* **1982**, *38*, 3909.

S0002-7863(97)03017-5 CCC: $15.00 © 1998 American Chemical Society
Published on Web 04/11/1998

Scheme 3

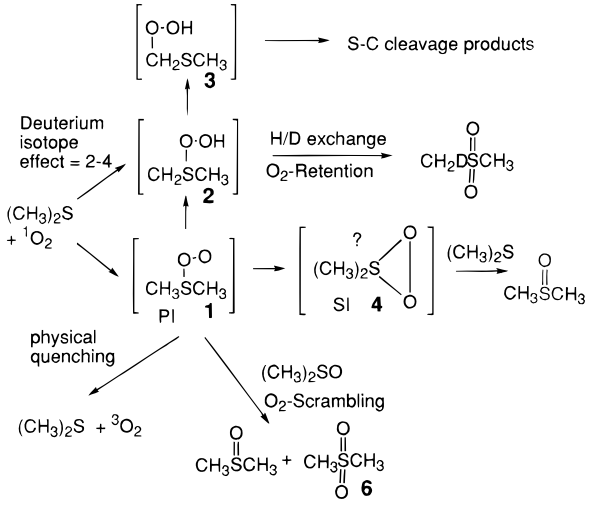

Ishiguro et al.[12] have recently shown that H−D exchange can accompany sulfone formation in the reaction of dimethyl sulfide with singlet oxygen in aprotic solvents (Scheme 3) and that *both* oxygens of singlet oxygen are incorporated into the sulfone (i.e. no O_2 scrambling). An isotope effect (k_H/k_D) of between 2 and 4 was measured[12] for the rate-determining step (RDS) of H/D-exchangeable sulfone formation. In addition, an isotope effect of 4.3 was measured[12] for benzaldehyde formation from $^1O_2$ and PhSCHDPh. A mechanism is presented in Scheme 3 (structures with boldface numbers are given in Figure 1) that is slightly modified from that of Ishiguro et al.[12] The large isotope effect for the RDS of H/D-exchangeable sulfone formation and S−C cleavage might suggest that both pathways go through a common intermediate.

The PM3 semiempirical treatment[16] was used by Ishiguro et al.[12] to compute activation enthalpies from $(CH_3)_2SOO$ (**1**). The intermediate $CH_3S(CH_2)OOH$ (**2**) was formed with a barrier of 18.9 kcal/mol by α-proton abstraction from $(CH_3)_2SOO$ (**1**). From $CH_3S(CH_2)OOH$ (**2**), two transition states were located. The lower energy one ($\Delta H_a = 14.9$ kcal/mol) yielded CH_3SCH_2OOH (**3**) while the higher energy transition state ($\Delta H_a = 25.5$ kcal/mol) yielded $CH_3S(CH_2)(O)OH$ (**5**). The relative barriers are not consistent with experiment since sulfone formation (which is experimentally observed) is not likely to result from CH_3SCH_2OOH (**3**).

Several of the radicals considered in fragmentation reactions of $(CH_3)_2SOO$ (including CH_3SCH_2, CH_3SCH_2O, and CH_3SCH_2OO) as well as closed-shell species (including CH_3SCH_2OOH and $CH_3SC(O)H$) have also been of interest in the atmospheric oxidation of dimethyl sulfide (see eqs 1−5).[17−23] Thus, some of the reactions considered in the present study of unimolecular reactions of $(CH_3)_2SOO$ will also be of relevance in the atmospheric oxidation of $(CH_3)_2S$.

$$(CH_3)_2S + OH \rightarrow CH_3SCH_2 + H_2O \quad (1)$$

$$CH_3SCH_2 + O_2(\text{triplet}) \rightarrow CH_3SCH_2OO \quad (2)$$

$$CH_3SCH_2OO + O_2H \rightarrow CH_3SCH_2OOH + O_2(\text{triplet}) \quad (3)$$

$$CH_3SCH_2OOH \rightarrow CH_3SC(O)H + H_2O \quad (4)$$

$$CH_3SCH_2OO + NO \rightarrow CH_3SCH_2O + NO_2 \quad (5)$$

Computational Method

The density functional theory exchange/correlation combination of B3/LYP has been used with the 6-31+G(d) basis set for geometry optimization. This level of theory has proven to be effective in reproducing geometries in a wide variety of bonding environments.[24,25] In addition, Jensen et al.[3b] have optimized a number of the same structures considered in the present work at the MP2/6-31G(d) level and have found reasonable agreement with B3LYP/6-31+G(d) geometries. Vibrational frequencies have been computed at the B3LYP/6-31+G(d) level to confirm the nature of the stationary points and to make zero-point corrections. The imaginary frequency (transition vector) was plotted for all transition states to ensure that the motion was appropriate for converting reactants to products. This was the case for all transition states except **TS2/5**. Single-point calculations have been made at QCISD(T)/6-31+G(d) and MP2/6-311+G(3df,2p) and combined with the additivity approximation to estimate relative energies at the [QCISD(T)/6-311+G(3df,2p)] level (eq 6).

$$\Delta E(\text{QCISD(T)/6-311+G(3df,2p)}) \approx \Delta E(\text{QCISD(T)/6-31+G(d)}) + \Delta E(\text{MP2/6-311+G(3df,2p)}) - \Delta E(\text{MP2/6-31+G(d)}) + \Delta(\text{ZPC/B3LYP/6-31+G(d)}) + \Delta\text{HLC} \quad (6)$$

The approximation in eq 6 is similar to the G2(MP2,SVP) procedure[26] except that the 6-31+G(d) basis set replaces the 6-31G(d) basis set in the QCISD(T) calculation. The G2(MP2,SVP) method has been shown by Radom and co-workers[26a] to reproduce a number of molecular properties to within chemical accuracy (2 kcal/mol). The difference in the higher level correction term (ΔHLC), obtained from G2 theory,[27] is zero except when the number of α and β spin electrons is different from the reference compound. For example, forming two radical fragments from the reference compound, $CH_3S(CH_2)OOH$ (**3**) will have a contribution of 3.1 kcal/mol (ΔHLC) added to the relative energy due to the difference in the number of α and β electrons. The higher level correction accounts for known deficiencies in the target computational level (QCISD(T)/6-311+G(3df,2p)).[27]

The primary intermediate, $(CH_3)_2SOO$ (**1**), proved to be problematic for the DFT method. The only minimum that could be obtained was characterized by a S−O bond distance of 2.359 Å and an O−O distance of 1.266 Å. The trouble can be traced to the fact that the reaction $(CH_3)_2SOO \rightarrow (CH_3)_2S + O_2$ is exothermic and no barrier exists at the

(16) Stewart, J. J. P. *J. Comput. Chem.* **1989**, *10*, 209.
(17) Wallinton, T. J.; Ellermann, T.; Nielse, O. J. *J. Phys. Chem.* **1993**, *97*, 8442.
(18) Butkovskaya, N. I.; LeBras, G. *J. Phys. Chem.* **1994**, *98*, 2582.
(19) Patroescu, I. V.; Barnes, I.; Becker, K. H. *J. Phys. Chem.* **1996**, *100*, 17207.
(20) Lacombe, S.; Loudet, M.; Banchereau, E.; Simin, M.; Pfister-Guillouzo, G. *J. Am. Chem. Soc.* **1996**, *118*, 1131 and references therein.
(21) Hung, W.-C.; Shen, M.; Lee, Y.-P.; Wang, N.-S.; Cheng, B.-M. *J. Chem. Phys.* **1996**, *105*, 7402.
(22) Nielsen, O. J.; Sehested, J.; Wallington, T. J. *Chem. Phys. Lett.* **1995**, *236*, 385.
(23) McKee, M. L. *Chem. Phys. Lett.* **1994**, *231*, 257.
(24) Bartolotti, L. J.; Flurchick, K. An Introduction to Density Functional Theory. In *Reviews in Computational Chemistry*; Lipkowitz, K. B., Boyd, D. B., Eds.; VCH: New York, 1996; Vol. 7.
(25) Frisch, M. J.; Trucks, G. W.; Schlegel, H. B.; Gill, P. M. W.; Johnson, B. G.; Robb, M. A.; Cheeseman, J. R.; Keith, T.; Petersson, G. A.; Montgomery, J. A.; Raghavachari, K.; Al-Laham, M. A.; Zakrzewski, V. G.; Ortiz, J. V.; Foresman, J. B.; Cioslowski, J.; Stefanov, B. B.; Nanayakkara, A.; Challacombe, M.; Peng, C. Y.; Ayala, P. Y.; Chen, W.; Wong, M. W.; Andres, J. L.; Replogle, E. S.; Gomperts, R.; Martin, R. L.; Fox, D. J.; Binkley, J. S.; Defrees, D. J.; Baker, J.; Stewart, J. P.; Head-Gordon, M.; Gonzalez, C.; Pople, J. A. Gaussian94 (Rev. B.1); Gaussian, Inc.: Pittsburgh, PA, 1995.
(26) (a) Smith, B. J.; Radom, L. *J. Phys. Chem.* **1995**, *99*, 6468. (b) Curtiss, L. A.; Redfern, P. C.; Smith, B. J.; Radom, L. *J. Chem. Phys.* **1996**, *104*, 5148. (c) Nicolaides, A.; Rauk. A.; Glukhovtsev, M. N.; Radom, L. *J. Phys. Chem.* **1996**, *100*, 17460.
(27) (a) Curtiss, L. A.; Raghavachari, K.; Trucks, G. W.; Pople, J. A. *J. Chem. Phys.* **1991**, *94*, 7221. (b) Curtiss, L. A.; Raghavachari, K.; Trucks, G. W. In *Quantum Mechanical Electronic Structure Calculations with Chemical Accuracy*; Langhoff, S. R., Ed.; Kluwer Academic: The Netherlands, 1995. (c) Raghavachari, K.; Curtiss, L. A. In *Modern Electronic Strcture Theory*, Yarkony, D. R., Ed.; World Scientific: Singapore, 1995.

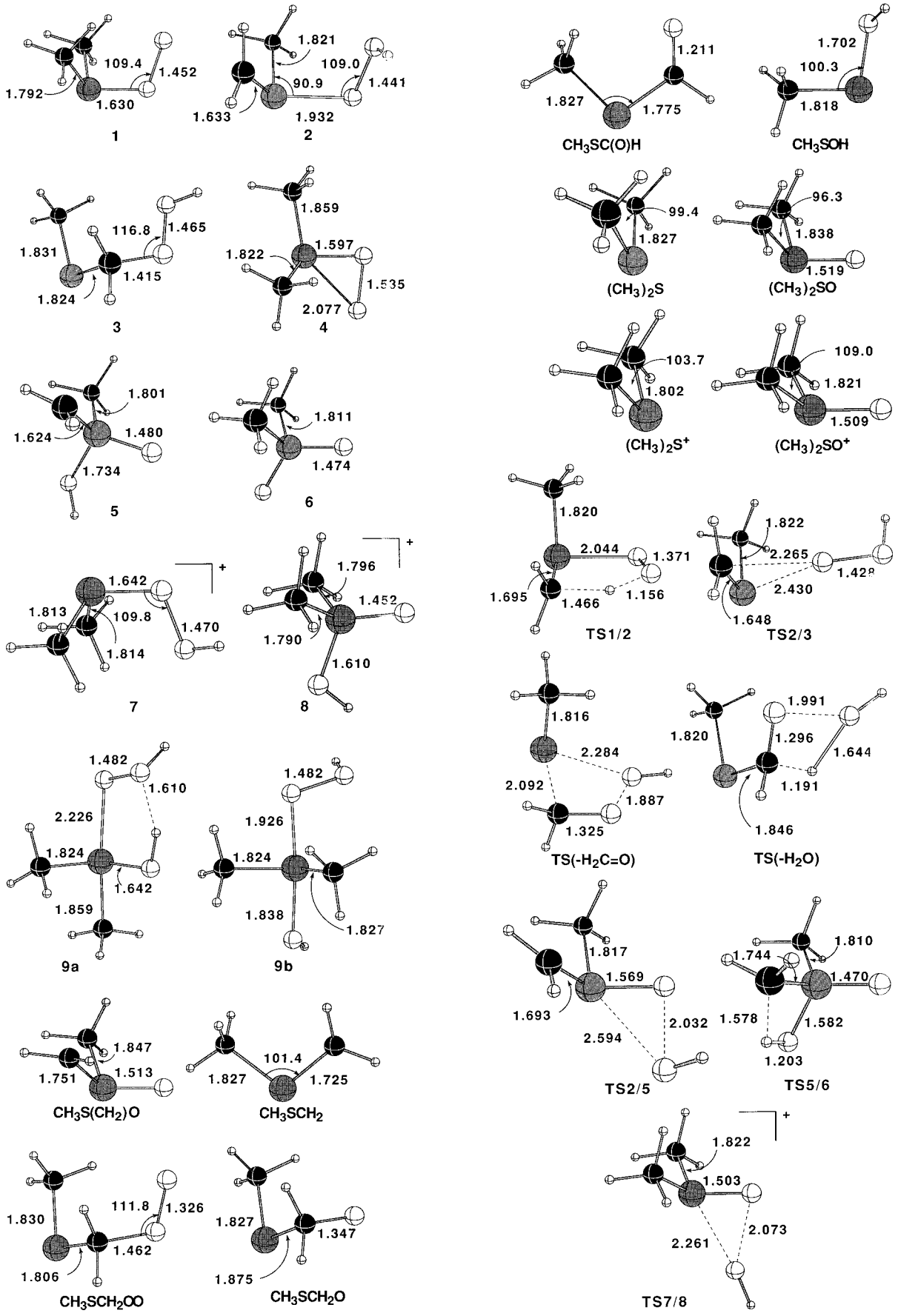

Figure 1. Selected geometric parameters for relevant species optimized at the B3LYP/6-31+G(d) level except for $(CH_3)_2SOO$ (**1**), which was optimized at the MP2/6-31+G(d) level.

Table 1. Relative Energies (kcal/mol) of Species on the $(CH_3)_2SOO$ (**1**−**6**), $(CH_3)_2SOOH^+$ (**7**, **8**), and $(CH_3)_2S(OH)OOH$ (**9**) Potential Energies Surfaces[a]

	B3LYP/a (+ZPC)	MP2/a	QCISD(T)/a	MP2/b	[QCISD(T)/b] (+ZPC/HLC)
$S(CH_3)_2 + O_2$ ($^1\Delta$)	−10.0 (−11.2)	−4.7	−6.5	4.2	2.4 (4.3)[b]
$(CH_3)_2SOO$ (**1**)		9.6	4.4	10.3	5.1 (5.3)
$CH_3S(CH_2)OOH$ (**2**)	0.0 (0.0)	0.0	0.0	0.0	0.0 (0.0)
CH_3SCH_2OOH (**3**)	−43.4 (−41.8)	−41.9	−44.0	−37.5	−39.6 (−38.0)
$(CH_3)_2SOO$ (**4**)	12.2 (12.5)	12.2	7.4	10.7	5.9 (6.2)
$CH_3S(CH_2)(O)OH$ (**5**)	−29.2 (−29.0)	−35.9	−30.2	−54.1	−48.4 (−48.2)
$(CH_3)_2SO_2$ (**6**)	−75.4 (−73.1)	−84.5	−78.5	−101.9	−95.9 (−93.6)
TS1/2	9.0(6.4)	6.7	12.6	6.8	12.7 (10.1)
TS2/3	14.1 (13.3)	18.7	14.6	21.9	17.8 (17.0)
TS(−H_2C=O)	11.2 (10.0)	12.2	7.5	17.2	12.5 (11.3)
TS(−H_2O)	4.4 (1.6)	7.1	2.8	11.3	7.0 (4.2)
TS2/5	50.6 (47.6)	48.2	14.7	44.8	11.3 (8.3)
TS5/6	−11.5 (−13.2)	−17.2	−10.9	−38.4	−32.1 (−33.8)
$CH_3S(CH_2)O + OH$	11.2(6.1)	25.4	19.8	22.5	16.9 (14.9)[b]
$CH_3SCH_2 + O_2H$	16.4 (12.7)	33.3	21.7	38.9	27.3 (26.7)[b]
$CH_3SCH_2OO + H$	40.6 (35.0)	43.7	35.8	57.2	49.3 (46.8)[b]
$CH_3SCH_2O + OH$	−5.3 (−8.7)	10.4	−3.3	17.9	4.2 (3.9)[b]
$CH_3SOH + H_2C$=O	−72.6 (−74.4)	−72.5	−72.8	−69.8	−70.1 (−71.9)
CH3SC(O)H + H_2O	−104.3 (−106.1)	−106.8	−104.9	−107.0	−105.1 (−106.9)
$(CH_3)_2SOOH^+$ (**7**)	0.0 (0.0)	0.0	0.0	0.0	0.0 (0.0)
$(CH_3)_2S(O)OH^+$ (**8**)	−34.8 (−34.0)	−43.5	−36.0	−60.4	−52.9 (−52.1)
TS7/8	50.8 (48.9)	42.5	40.7	39.6	37.8 (37.7)
$(CH_3)_2SO^+ + OH$	37.2 (32.8)	51.3	39.5	50.7	38.9 (37.6)[b]
$(CH_3)_2S^+ + O_2H$	39.4 (35.8)	53.3	44.5	61.3	52.5 (48.4)[b]
$(CH_3)_2SOO$ (**1**) + H_2O		0.0	0.0	0.0	0.0 (0.0)
$(CH_3)_2S(OH)OOH$ (**9a**)		−7.3	−4.8	−7.5	−5.0 (−1.7)
$(CH_3)_2S(OH)OOH$ (**9b**)		−22.7	−17.8	−21.8	−16.9 (−13.5)

[a] Basis set "a" is 6-31+G(d); basis set "b" is 6-311+G(3df,2p). [b] The higher level correction (HLC) increases the energy by 3.1 kcal/mol relative to **2**.

DFT level. In contrast, a barrier to dissociation exists at the MP2/6-31+G(d) level, and a stable structure can be obtained. A similar deficiency in the DFT method was also observed for the ONOO radical.[28] For that reason, the structure and vibrational frequencies of **1** were obtained at MP2/6-31+G(d) rather than the B3LYP/6-31+G(d) level. The MP2/6-31+G(d) zero-point energy of **1** was scaled by the B3LYP:MP2 ratio calculated for the zero-point energy of $(CH_3)_2S$.

Rather than calculate singlet O_2 directly (which would require a complex wave function), the ground-state triplet was computed and the experimental singlet−triplet separation of 22.0 kcal/mol[29] was added. A table of energies (in kcal/mol) relative to $CH_3S(CH_2)OOH$ (**2**) is presented in Table 1 while geometries of relevant species are given in Figure 1. Total energies, zero-point energies, and Cartesian coordinates of optimized structures are available as Supporting Information. Unless otherwise stated, relative energies will be determined from eq 6. The reaction profile for $(CH_3)_2S + {}^1O_2$ is given in Figure 2 while the reaction **7** → **8** is given in Figure 3. Vertical arrows in Figures 2 and 3 refer to bond dissociation energies.

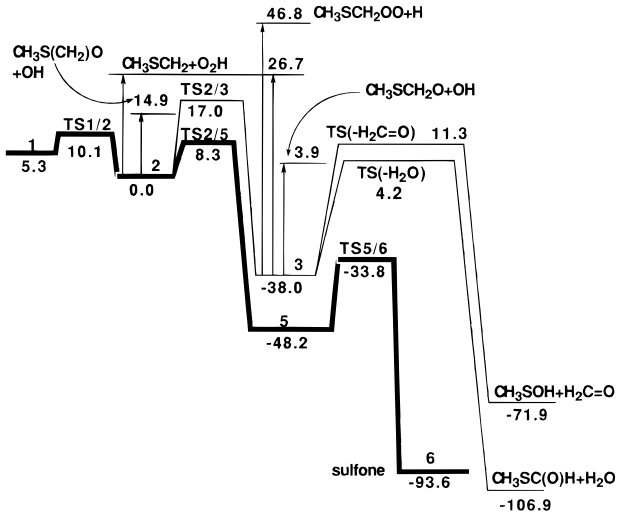

Figure 2. Unimolecular reactions on the $(CH_3)_2SOO$ (**1**) potential energy surface. Vertical arrows indicate bond cleavage reactions. The bold line indicates the formation of dimethyl sulfone (**6**) from $(CH_3)_2SOO$ (**1**). Structures of stationary points are given in Figure 1.

Results and Discussion

As mentioned above, the structure of $(CH_3)_2SOO$ (**1**) was optimized at the MP2/6-31+G(d) level rather than the B3LYP/6-31+G(d) level because the length of the S−O bond is much too long with use of DFT. At the MP2/6-31+G(d) level, the S−O bond is 1.630 Å and the O−O bond is 1.452 Å. The dissociation reaction to form $(CH_3)_2S$ and triplet oxygen is 36.3 kcal/mol exothermic, which is reduced to 14.3 kcal/mol if singlet oxygen is the reference product. At the [QCISD(T)/6-311+G(3df,2p)] level, the difference is reduced further from 14.3 to 2.7 kcal/mol. The ΔHLC term reduces the difference by a further 3.1 kcal/mol because the computations are with respect to triplet oxygen and $(CH_3)_2S$ for which the number of α and β electrons is different than in $(CH_3)_2SOO$. The difference is increased by 1.4 kcal/mol from zero-point corrections to bring the final separation to 1.0 kcal/mol (Table 1). It is likely that solvent effects will further stabilize the zwitterionic structure $(CH_3)_2SOO$ (relative to $(CH_3)_2S$ and O_2) in protic solvents such as methanol and to a smaller degree in aprotic solvents such as benzene and acetonitrile.

The calculated B3LYP/6-31+G(d) geometry of thiadioxirane (**4**) is similar to that reported by Jensen[30] at the MP2/6-31G(d) level except the S−O distances which are more asymmetric with DFT (01.597/2.077 Å, B3LYP/6-31+G(d); 1.648/1.809 Å, MP2/6-31G(d)). The present study finds the reaction **1** → **4** to be

(28) McKee, M. L. *J. Am. Chem. Soc.* **1995**, *117*, 1629.

(29) Cotton, F. A.; Wilkinson, G. *Advanced Inorganic Chemistry*, 5th ed.; Wiley: New York, 1988.

(30) Jensen, F. *J. Org. Chem.* **1992**, *57*, 6478.

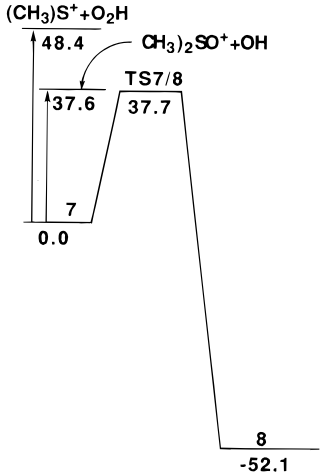

Figure 3. Unimolecular reaction of $(CH_3)_2SOOH^+$ (**7**) to form $(CH_3)_2S(O)OH^+$ (**8**). Vertical arrows indicate bond cleavage reactions. Structures of stationary points are given in Figure 1.

slightly endothermic (0.9 kcal/mol), which compares to a value of 0.4 kcal/mol for the reaction at the MP4/6-311G(2d)+ZPC level.[30] Due to the aforementioned difficulties with **1**, the rearrangement **1** → **4** was not calculated. However, it should be mentioned that Jensen has calculated[30] a sizable barrier for this reaction at the MP4/6-311G(2d)+ZPC level (18.6 kcal/mol). Very recent calculations by Shangguan and McAllister[31] of the relative energies of **1** and **4** are in agreement with those of Jensen.[30]

It is known that sulfides with an active α-proton lead to S−C cleavage products, probably through intramolecular hydrogen abraction.[4,5] More recent results indicate that a fraction of the sulfone produced in the photolytic oxidation of sulfides occurs with H/D exchange along with incorporation of both oxygen atoms of molecular oxygen.[12] There is an isotope effect of $k_H/k_D = 2-4$ for the production of this fraction of sulfones which suggests that the rate-determining step involves C−H bond breaking.[12] A transition state for hydrogen abstraction (**TS1/2**) was located (Figure 1) with an activation barrier of only 4.8 kcal/mol. Since the transition state was located at the B3LYP/6-31+G(d) level, the structure may be plagued by the same difficulties discussed above for $(CH_3)_2SOO$ (**1**); that is, the S−O bond may be too long and the O−O bond too short. A more difficult question to answer is whether the product, $CH_3S(CH_2)OOH$ (**2**), might be formed directly from $(CH_3)_2S$ and singlet oxygen. At the DFT level of theory, an intrinsic reaction path (IRP) would not help resolve this issue due to the poor description of **1**. The yield of sulfone is known to be independent of the addition of diphenyl sulfoxide, a known trap of persulfoxide.[4] This fact suggests the persulfoxide and the sulfone-producing intermediate are produced by independent pathways.

If $(CH_3)_2S + {}^1O_2$ and **1** are in rapid equilibrium, and **TS1/2** is the transition state of the rate-determining step, then the expression for the observed rate constant is given in Scheme 4.[4,7] Thus, there is a contribution from the reaction energy of $(CH_3)_2S + {}^1O_2$ to **1** (1.0 kcal/mol) and the activation enthalpy from **1** → **2** (4.8 kcal/mol) for a total activation barrier of 5.8 kcal/mol. An experimental activation barrier for singlet oxygen reaction with cyclic pentamethylene sulfide of −4.1 kcal/mol had been determined[7] in acetone. A stabilization effect of the solvent on **1** and **TS1/2** could account for the negative activation barrier. The computed entropy of activation for $(CH_3)_2S + {}^1O_2$ → **2** has a large contribution from the associate reaction ($(CH_3)_2S + {}^1O_2$ → **1**, −36.7 cal/(mol·K)) and a much smaller contribution from **1** → **TS1/2** (−1.2 cal/(mol·K)). The total entropy change (−36.7 cal/(mol·K)) is in reasonable agreement with the experimental entropy of activation for photooxidation of *c*-$(CH_2)_5S$ of −46 cal/(mol·K).

Scheme 4

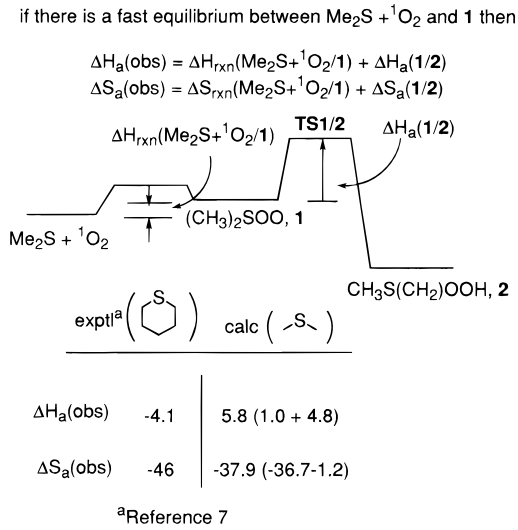

The intermediate **2** has a rather short S−C bond to methylene (1.633 Å) that is indicative of double-bond character. The O−O bond distance (1.441 Å) and O−O torsion angle (99.9°) are in the normal range of O−O peroxide distances and torsion angles.[29] Two low-energy fragmentation pathways are considered from **2**, cleavage of the S−O bond to give $CH_3SCH_2 + O_2H$ (26.7 kcal/mol) and cleavage of the O−O bond to give $CH_3S(CH_2)O + OH$ (14.9 kcal/mol). In both sulfur-containing radical fragments, the unpaired electron density shifts almost completely to the methylene carbon. This S−C bond then lengthens from 1.633 Å in **2** to 1.725 Å in CH_3SCH_2 and 1.751 Å in $CH_3S(CH_2)O$ (Figure 1). The O−O bond dissociation energy in **2** of 14.9 kcal/mol gives the upper limit of the rearrangement barrier to $CH_3S(CH_2)(O)OH$ (**5**) since that would correspond to a two-step process where the O−O bond breaks completely before the S−OH bond forms. A transition state for OH migration **2** → **5** was located at the B3LYP/6-31+G(d) level (**TS2/5**, Figure 1) where the breaking O−O bond is 2.032 Å and the forming S−OH bond is 2.594 Å. The fact that the energy of **TS2/5** is 41.6 kcal/mol higher than that of the fragments, $CH_3S(CH_2)O + OH$, indicates that the B3LYP/6-31+G(d) method is not able to fully describe the biradical character of the transition state. The QCISD(T)/6-31+G(d) level makes a dramatic difference to the barrier, reducing it 33.5 kcal/mol compared to the MP2/6-31+G(d) level. At the standard level of theory, the barrier is 8.3 kcal/mol, 6.6 kcal/mol less than the energy of fragments. A search for the transition state at the CASSCF(2,2)/6-31G(d) level starting with a broken symmetry solution of the wave function revealed a flat potential energy surface with a weakly interacting OH group. It is probable that a method which can describe dynamic and nondynamic electron correlation will be needed to locate the transition state. At the QCISD/6-31+G(d) level, the transition state energy of **TS2/5** is still considerably above that of radical fragments, indicating the importance of triple excitations. In any event, it is clear that the low barrier for OH migration in **2** is directly related to the small O−O bond energy which should be accurately calculated.

(31) Shangguan, C.; McAllister, M. A. *THEOCHEM* **1998**, *422*, 123.

Scheme 5

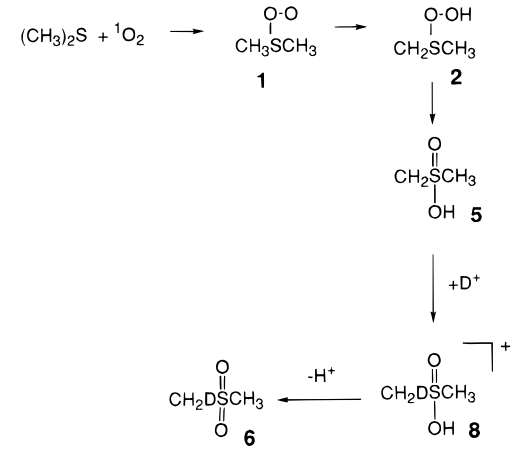

Table 2. Proton Affinities (kcal/mol) of H_2O, **1**, **2**, **5**, and **6**[a]

	B3LYP/a (+ZPC)	MP2/a	QCISD (T)/a	MP2/b	[QCISD(T)/b][b] (+ZPC)
$H_2O \rightarrow H_3O^+$	167.2 (158.9)	168.1	169.2	169.9	171.0 (162.7)
1 → **7**		243.7	242.6	245.8	244.7 (236.9)
2 → **7**	237.9 (227.3)	234.0	238.2	235.7	239.9 (229.3)
5 → **8**	243.5 (234.9)	241.6	244.0	242.0	244.4 (235.8)
6 → **8**	197.3 (190.8)	193.0	195.7	194.1	196.8 (190.3)

[a] Basis set "a" is 6-31+G(d); basis set "b" is 6-311+G(3df,2p). [b] Addititivity approximation. See eq 6.

The p orbital on the methylene carbon in **TS2/5** is aligned with the forming S═O bond which should allow conjugation to take place. However, after the OH has transferred to the sulfur, the methylene reorientates so the π^* orbital can interact with the hydroxyl lone pair. The twisting of the methylene group as the reaction proceeds from **2** to **5** was also noted at the PM3 level by Ishiguro et al.[12] It is interesting to note that the S−C distance to the methylene carbon remains rather short as one proceeds from **2** (1.633 Å) to **TS1/2** (1.695 Å) to **5** (1.624 Å), which is in contrast to the S−C distance in the $CH_3S(CH_2)O$ fragment where it has increased to 1.751 Å. Evidently, the S−CH_2 retains considerable double bond character through the reaction.

The reaction forming $CH_3S(CH_2)(O)OH$ (**5**) from **2** is exothermic by 48.2 kcal/mol, which should make this step irreversible (Figure 2). In turn, structure **5** is connected to dimethyl sulfone (**6**) via **TS5/6** with a barrier of 14.4 kcal/mol. The transition state for reaction **5** → **6** is rather early as judged (Figure 1) by the short breaking O−H bond (1.203 Å) and long forming C−H (1.578 Å) in keeping with a reaction that is 48.2 kcal/mol exothermic (Figure 2).

If the reaction followed the bold line in Figure 2 to dimethyl sulfone (**6**), the reaction would not involve H/D exchange since the same hydrogen that is abstracted to form **2** is transferred back to form **6**. This would be in contradiction to experiment[12] as it is known that H/D from adventitious water exchanges with one of the six hydrogens of dimethyl sulfide. To rationalize the exchange (Scheme 5), it is assumed that **5** is protonated on the methylene group to form $(CH_3)_2S(O)OH^+$ (**8**). The proton affinity of **5** is calculated to be 235.8 kcal/mol, which is 73.1 kcal/mol greater than that of water (Table 2). If **8** is now deprotonated on oxygen, dimethyl sulfone (**6**) is formed with one H/D exchanged. Thus, the reaction **5** → **6** is acid catalyzed (**5** + H^+ → **8** → **6** + H^+).

The experimental results could also be explained if the protonation occurred earlier in the reaction scheme. Since the proton affinity of **2** (229.3 kcal/mol, Table 2) to form $(CH_3)_2SOOH^+$ (**7**) is similar to the proton affinity of **5** to form **8** (235.8 kcal/mol), it is possible that OH migration could take place in protonated **2**. This transition state (**TS7/8**) has a breaking O−O bond of 2.073 Å and a forming S−OH bond of 2.261 Å. The effect of electron correlation is not as dramatic for **TS7/8** as was noted above for **TS2/5**, which might suggest that there is less biradical character. The activation barrier for **7** → **8** is 37.7 kcal/mol, which is essentially the same as the energy of fragments $(CH_3)_2SO^+$ + OH (37.6 kcal/mol). Compared to the barrier for OH migration in **2** (8.3 kcal/mol), the barrier for OH migration in **7** (37.6 kcal/mol) is 29.3 kcal/mol higher. The difference is clearly attributable to the smaller O−O bond energy in **2** (14.9 kcal/mol) compared to the O−O bond energy in **7** (37.7 kcal/mol) which, in turn, is related to the effect of the methylene group.

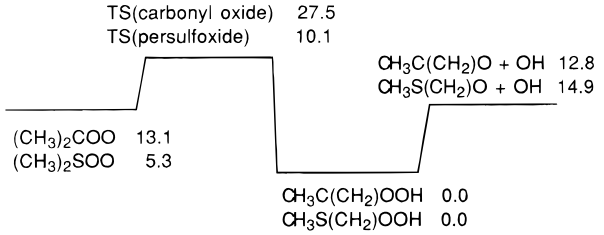

Figure 4. Comparison of 1,4-hydrogen migration barriers in dimethylcarbonyl oxide ($(CH_3)_2COO$) calculated at the B3LYP/6-31G(d,p) level plus zero-point and thermal corrections[32] with dimethyl sulfoxide ($(CH_3)_2SOO$) calculated in this work. Energies (in kcal/mol) are referenced to the indicated reactant plus singlet oxygen.

It has been previously noted[5] that carbonyl oxide has a reactivity similar to that of persulfoxide. Very recently, Gutbrod et al.[32] have reported theoretical calculations on dimethylcarbonyl oxide ($(CH_3)_2COO$) which indicate that 1,4-hydrogen migration can occur with a low barrier to form a hydroperoxide intermediate similar to that calculated here for $(CH_3)_2SOO$. The next step, which has been experimentally verified,[32b] is cleavage of the O−O bond to form hydroxyl radicals. The similarity of the reaction profiles for the initial stage of reaction is illustrated in Figure 4.

Another section of the potential energy surface is accessible via **TS2/3**, the transition state for migration of the peroxide group from sulfur (**2**) to the methylene carbon (**3**). The O_2H-migration transition state (**TS2/3**) is 8.7 kcal/mol above that of **TS2/5** and 9.7 kcal/mol below the energy of CH_3SCH_2 + O_2H fragments (Figure 2). Replacing methyl with other groups on the sulfide could reduce the energy between **TS2/3** and **TS2/5**, which could lead to products via the former pathway.

The CH_3SCH_2OOH intermediate (**3**) has been invoked in the mechanism of atmospheric oxidation of dimethy sulfide.[18] The O−O distance (1.465 Å) and torsion angle around the O−O bond (138.7°) in **3** are typical of peroxide compounds.[29] Three different fragmentation processes are considered for **3**: breaking the O−O bond to form CH_3SCH_2O + OH (41.9 kcal/mol), breaking the C−O bond to form CH_3SCH_2 + O_2H (64.7 kcal/mol), and breaking the O−H bond to form CH_3SCH_2OO + H (84.8 kcal/mol). The O−O bond is the weakest; its cleavage is competitive with two concerted elimination transition states. Elimination of water to form $CH_3SC(O)H$ + H_2O has a barrier of 42.2 kcal/mol via **TS(−H_2O)** and the elimination of formaldehyde to form CH_3SOH + H_2C═O has a barrier of 49.3 kcal/mol via **TS(−H_2C═O)**. The second reaction is observed

(32) (a) Gutbrod, R.; Schindler, R. N.; Kraka, E.; Cremer, D. *Chem. Phys. Lett.* **1996**, *252*, 221. (b) Gutbrod, R.; Kraka, E.; Schindler, R. N.; Cremer, D. *J. Am. Chem. Soc.* **1997**, *119*, 7330.

in the reaction of singlet oxygen with benzyl or cyclic sulfides, both of which lead to S−C cleavage reactions.[4,13] Ishiguro et al.[12] suggest that if there is a phenyl substitutent on carbon in transition state **TS2/5**, then the methylene group might not be able to assume the most stabilizing orientation, and the transition state would be destabilized as a consequence. In that event, **TS2/3** might become lower than **TS2/5** (or at least competitive with), which would lead to **3** (and S−C cleavage products) rather than **5** (and sulfones).

Perhaps more difficult to explain is the absence of products from **TS(−H_2O)** since that barrier is 7.1 kcal/mol lower than **TS(−H_2C═O)**. The reaction has been proposed[19] as a major channel in the reaction of O_2H with CH_3SCH_2OO (eq 7) but (to the author's knowledge) has not been observed in the reaction

$$CH_3SCH_2OO + O_2H \longrightarrow \begin{array}{l} CH_3SCH_2OOH + O_2 \\ \quad\quad\quad\quad\quad\quad \longrightarrow CH_3SC(O)H + H_2O \end{array} \qquad (7)$$

of singlet oxygen with sulfides. The transition state **TS(−H_2O)** can best be visualized as the cleavage of the O−O bond in **3** with the simultaneous abstraction of a C−H hydrogen by the departing hydroxyl radical. This reaction may be disfavored by entropy effects since the energy of the fragments (CH_3SCH_2O + OH) is already 0.3 kcal/mol lower (Figure 2) in energy than **TS(−H_2O)**.

In protic solvents such as methanol, photolytic oxidation of sulfides proceeds by a different mechanism after the persulfoxide is formed.[3,33−36] It has been suggested that a solvent molecule may complex to the persulfoxide or even add to form a sulfurane.[3,33−36] The energetics of the addition product was considered in $(CH_3)_2S(OH)OOH$ (**9**) (Figure 1) where two alternative structures were considered. In **9a**, the OH from water adds to an equatorial position around sulfur, which permits a strong hydrogen bond between OH and O_2H (1.610 Å). It appears that the preference of electronegative groups to assume axial positions is more important than the intramolecular hydrogen bond since **9b** (where OH is axial) is 11.8 kcal/mol more stable than **9a**. Relative to $(CH_3)_2SOO$ (**1**) plus water, **9b** is 13.5 kcal/mol more stable. Jensen has reported[3] an MP2/6-31G(d) optimized geometry for the addition product of methanol and $(CH_3)_2SOO$ (**1**) in which the OCH_3 group also adopts an axial position.

(33) Clennan, E. L.; Yang, K. *J. Am. Chem. Soc.* **1990**, *112*, 4044.
(34) Clennan, E. L.; Yang, K. *Tetrahedron Lett.* **1993**, *34*, 1697.
(35) Clennan, E. L.; Greer, A. *J. Org. Chem.* **1996**, *61*, 4793.
(36) Miller, B. L.; Williams, T. D.; Schöneich, C. *J. Am. Chem. Soc.* **1996**, *118*, 11014.

Conclusions

The reaction of singlet oxygen with dimethyl sulfide has proved to be deceptively complex. The present work, which considers unimolecular reactions from the primary intermediate, $(CH_3)_2SOO$ (**1**), confirms the importance of $CH_3S(CH_2)OOH$ (**2**) formed by intramolecular hydrogen abstraction with a barrier of only 4.8 kcal/mol. The O−O bond energy in $CH_3S(CH_2)$-OOH (**2**) is very weak (14.9 kcal/mol), which rationalizes the small activation barrier (8.3 kcal/mol) for forming $CH_3S(CH_2)$-(O)OH (**5**). An intramolecular hydrogen migration from the hydroxyl to the methylene group in **5** forms $(CH_3)_2SO_2$ (**6**) with a barrier of 14.4 kcal/mol. Alternatively, trace water can protonate the methylene group in **5**, which can, in turn, deprotonate on oxygen to form $(CH_3)_2SO_2$ (**6**). The acid-catalyzed pathway explains the single H/D exchange observed experimentally. With an additional 8.7 kcal/mol of activation, **2** can form CH_3SCH_2OOH (**3**), which leads to S−C cleavage products.

Acknowledgment. Computer time was provided by the Alabama Supercomputer Network. I would like to thank Sun Microsystems Computer Corporation for the award of an Academic Equipment Grant and Frank Jensen for providing a preprint of ref 3b.

Supporting Information Available: Total energies (hartrees) at the B3LYP/6-31+G(d), QCISD(T)/6-31+G(d), and MP2/6-311+G(3df,2p) levels and zero-point energies (kcal/mol) at the B3LYP/6-31+G(d) level (Table S1) for various species and Cartesian coordinates for relevant structures optimized at the B3LYP/6-31+G(d) level (except for $(CH_3)_2SOO$ (**1**)) (Table S2) (10 pages, print/PDF). See any current masthead page for ordering information and Web access instructions.

JA973017Z